Extended Abstract submitted to Ocean Optics 2016 conference on 7th October 2016

New opportunities and challenges for high resolution remote sensing of water colour

Kevin Ruddick[1,*], Quinten Vanhellemont[1], Ana Dogliotti[2], Bouchra Nechad[1], Nicholas Pringle[1] and Dimitry Van der Zande[1]

[1]Royal Belgian Institute for Natural Sciences (RBINS), Operational Directorate Natural Environment, 100 Gulledelle, 1200 Brussels, Belgium.
[2]Instituto de Astronomía y Física del Espacio (IAFE), CONICET/UBA, Argentina
*Corresponding author, Email: kruddick@naturalsciences.be

Abstract

The last two years have seen a dramatic increase in the applications of optical remote sensing for turbid coastal and inland waters, driven largely by the availability of free, high quality and high resolution satellite data from Landsat-8 and Sentinel-2. It is now possible to regularly and systematically map the distribution and dynamics of suspended particles and certain impacts of human activities close to shore and inside ports, estuaries and inland waters. Commercial missions such as Pléiades, Worldview and Rapideye also offer new possibilities for remote sensing of aquatic processes at even higher spatial resolutions (~1m). The exploitation of such data brings new algorithmic challenges and opportunities including: the use of SWIR bands for atmospheric correction in turbid waters; the challenge of lower signal:noise specifications and possible spatial binning techniques; the exploitation of extremely high resolution panchromatic bands; the assessment of the impact of sub-pixel scale effects for medium resolution ocean colour missions; the need to remove/filter sunglint and surface wave effects; the possibility to resolve patchy distributions (suspended matter, surface foam, algal blooms, floating vegetation, etc.); problems of data contamination by cloud and object shadows; and the validation of narrow swath sensors. The state of the art of high resolution remote sensing of water colour is reviewed here and the many emerging opportunities and algorithmic challenges are outlined using examples from Landsat-8, Sentinel-2 and Pléiades.

1. Introduction

"Ocean Colour" remote sensing, as implied by the name, used to be concerned with the processing and exploitation of remote sensing data of the oceans. This data generally derived from the "mainstream" ocean colour sensors, such as SeaWiFS, MODIS, MERIS, VIIRS and OLCI, with typical spatial resolution of 300m-1200m, approximately daily data, typically 8-18 spectral bands and a high signal noise ratio for accurate radiometric performance over dark water targets. Since the launch of SeaWiFS, there has been a growing interest in using such data for coastal and inland water applications because of the strong relevance to human activities. A new revolution has occurred thanks to the free and easily available high resolution data from Landsat-8 (30m multispectral, launched 2013-02-11) and Sentinel-2 (10-60m multispectral, launched 2015-06-23). Many new processes, particularly those relating to human activities, can be seen at 10-30m that were not previous visible at 300m. Some opportunities for new applications based on these datasets are described and the new challenges for data processing are summarised.

2. Application Opportunities

Improvement in spatial resolution from ~300m (OLCI) to ~30m (Landsat-8) or ~10m (Sentinel-2) makes possible remote sensing of many new human activities or impacts in coastal, estuarine and inland waters.

For example, for most large ports the spatial distribution of water properties such as suspended particulate matter (SPM) concentration cannot be mapped at 300m resolution, but can be resolved adequately with 30m resolution data or commercially-available 1-2m data. This opens up new possibilities for understanding sediment transport into/out of ports (**Figure 1**) and estuaries and optimising dredging and/or monitoring activities. The SPM around ports and other offshore constructions, such as wind farms (Q. Vanhellemont and Ruddick 2014), platforms and artificial islands, can also now be easily mapped and better understood. Indeed for many such constructions it is necessary to carry out an Environmental Impact Study and/or continuous monitoring, which may now be facilitated, for the aspects relating to suspended sediments and their transport, by remote sensing. The spatial extent of impacts from sand and gravel extraction (Van Lancker et al. 2013) can also be more easily understood. Dredging companies can use high resolution remote sensing to clearly establish natural sources of SPM and thus facilitate and demonstrate compliance with environmental regulations. Governmental authorities can use remote sensing to identify illegal SPM disposal activities (Vanhellemont and Ruddick 2015).

Whereas SPM mapping (including atmospheric correction) can be achieved with quite simple remote sensors, e.g. with a red band and a near infrared band (Stumpf and Pennock 1989; Neukermans et al. 2009), mapping of chlorophyll (CHL) sets more stringent requirements on the spectral band set. In turbid waters, where non-algae particle absorption can mask algae particle absorption in the blue-green spectral range, it is necessary to have spectral bands inside the red (~665nm) chlorophyll *a* absorption feature and just outside, e.g. 705-709nm, as on MERIS and OLCI. The Sentinel-2 band set does have bands at 665nm (10m) and 705nm (20m) which are appropriate for CHL mapping in turbid waters, thus offering an impressive improvement in spatial resolution from 300m (MERIS/OLCI) to 20m (Vanhellemont and Ruddick 2016; Toming et al. 2016), provided that radiometric noise at these bands does not degrade performance. This opens up new opportunities for CHL mapping close to the coast, which is useful for water quality reporting in the context of the European Union Water Framework Directive (Bresciani et al. 2011; Gohin et al. 2008), and in many estuaries, ports and inland waters.

A third family of commonly used aquatic parameters from optical remote sensing consists of parameters relating to underwater transparency or light attenuation, including monochromatic or spectral or broadband diffuse attenuation coefficient (“Kd”), euphotic depth, horizontal visibility, etc. (Doron et al. 2007). Such parameters are needed by, for example, ecosystem modellers (Lacroix et al. 2007), professional divers, and marine scientists, limnologists and managers of coastal and inland water quality managers. The higher spatial resolution offered by satellites such as Landsat-8 and Sentinel-2 may be of particular use to understanding small scale variability, e.g. around the bases of windmills where divers carry out monitoring or maintenance.

Extremely high biomass plankton blooms and floating vegetation and cyanobacteria scum (Dierssen, Chlus, and Russell 2015; Hu 2009; Matthews, Bernard, and Robertson 2012) are often patchy in space and much easier to detect at high spatial resolution, e.g. (Van Mol et al. 2007) and **Figure 2**. Floating vegetation can be both environmentally important, as a habitat for certain species, and of socio-economic importance, e.g. as a nuisance to shipping (Williams 2005).

Benthic vegetation and important habitats such as corals are also often patchy in space. There is a longstanding tradition of using remote sensors such as Landsat for mapping seagrass beds and corals (Dekker et al. 2006; Mumby et al. 1997). The release of free and easily available data from Landsat-8 and Sentinel-2 will dramatically improve the amount of imagery that can be used in such studies and hence improve understanding of any temporal variability of benthic habitats.

Finally, many manmade objects become visible at 10-30m including ships, offshore platforms, jetties, bridges, pipelines, aquaculture sites, etc. These objects may impact on the aquatic environment in diverse ways – the highest resolution data can show both the objects and the optical aspects of their environmental impact.

3. Scientific Opportunities

In addition to the new applications that have been developed from the now freely and easily available high resolution satellite data, there are new opportunities for improving observation, and hence scientific understanding, of small scale aquatic processes. For example, phytoplankton distributions may have significant patchiness at spatial scales of a few metres, which may be related to small scale physical-biological interactions (Franks and Walstad 1997). The patchiness of SPM at length scales of a few metres or less has been observed in many turbid estuaries and coastal waters (**Figure 3**). The physical processes causing such patchiness are not entirely clear. Oceanic and estuarine fronts are often marked by a sharp line of foam and/or floating debris because of convergence in surface currents (Bowman and Iverson 1978). The optical impacts of other physical processes occurring at scales between 1m and 300m, such as surface gravity waves, can now be measured very systematically.

Mass exploitation of high resolution optical imagery is likely to lead to a better understanding of such processes in their own right as well as a better representation of such subpixel scale effects in medium resolution ocean colour imagery. As an example of such potential, **Figure 4** shows near-simultaneous (62 seconds apart) imagery from two different viewing angles, one with strong sunglint, the other without.

4. Data Processing Challenges

The advent of mass processing of high resolution imagery for water bodies brings new challenges for data processing algorithms. There are currently no standard level 2 water products for missions such as Landsat or Sentinel-2 because these were designed only for land targets. However, free software is now available to perform an automated Atmospheric Correction (AC) for these sensors, e.g. ACOLITE, SeaDAS, BEAM/sen2cor.

At high spatial resolution, some processes that are subpixel scale for 300-1000m imagery become spatially resolved and require a different treatment:

Spatial variability of skyglint from wind waves and swell with typical length scales of 1-30m become very obvious in high resolution imagery because of the change in Fresnel reflectance associated with different skylight incidence angles, possibly combined with different brightnesses of the reflected sky – see **Figure 5**. The spatial average of such waves is generally removed from medium resolution imagery in the AC. An AC allowing pixel-by-pixel (PP) variation of aerosol (and skyglint) reflectance, e.g. by simple differencing of red and near infrared wavelengths, can be reasonably effective in removing skyglint from waves. However, PP AC algorithms will generally suffer from noise and AC algorithms for high noise sensors, such as L8 and S2, generally need some spatial smoothing of the atmospheric correction bands (Vanhellemont and Ruddick 2015; Vanhellemont and Ruddick 2016). Since both sensor noise and wind waves have length scales at or close to the pixel size but different spectral correlations (noise is spectrally uncorrelated, wave effects are spectrally correlated if bands are simultaneously acquired) it can be difficult to remove both wave effects and noise in the AC, while preserving the real spatial variability of water reflectance.

Spatial variability of sunglint also becomes very obvious in high resolution imagery if viewing close to the specular reflection direction, e.g. **Figure 4**. Sunglint can have very small spatial scales, e.g. cm capillary waves, and is not totally spatially resolved even in 1m imagery. The spectral variation of sunglint can be calculated on an image-by-image or moving window basis assuming that other processes (water, aerosols) have less variability at short length scales (Hochberg, Andrefouet, and Tyler 2003; Hedley, Harborne, and Mumby 2005). Using this information on the spectral variation of sunglint it is still necessary to estimate the amplitude of sunglint reflectance for each high resolution pixel. The problem here is quite similar to the problem of estimating the amplitude of aerosol and/or skyglint reflectance and can be approached by identifying a reference wavelength where water reflectance is known to be zero or easily calculated (Gordon and Wang 1994; Wang and Shi 2005; Quinten Vanhellemont and Ruddick 2015) or by multi-spectral inversion of a coupled water-atmosphere model (Steinmetz, Deschamps, and Ramon 2011).

Cloud shadows become much more problematic in high resolution imagery. At 300-1000m resolution cloud shadows are generally removed along with cloud edge pixels by simple spatial enlargement of detected clouds or are sometimes removed in dark waters as low radiance pixels. At 10-30m resolution such a crude approach would remove too much useful data and a less conservative approach would miss many cloud shadow contaminated pixels giving very bad data to users. Since cloud shadow pixels can look spectrally identical to other clear sky water pixels, spectral tests are insufficient for detection and it is necessary to use information on sun location and, if available, cloud height to project detected clouds horizontally to cloud shadow pixels. Such geometric algorithms can be combined with more complicated object search algorithms (Zhu and Woodcock 2012), although the latter can be confused by regions of high spatial variability of water reflectance. A reasonable approach (Pringle, N., Vanhellemont, Q., and Ruddick, K. 2015) seems to be to assume a conservatively high cloud top height, possibly higher for cirrus clouds, and project clouds away from sun, flagging all pixels as cloud shadow contaminated.

It is noted that cloud shadow pixels do contain information on the atmosphere and on water level direct/diffuse irradiance that might be useful for AC purposes (Chang et al. 2007). However, an operational AC algorithm cannot rely on the presence of cloud shadow pixels and the shadowing of atmospheric reflectance at different heights and the different transmittances of thick and thin clouds can complicate exploitation of cloud shadow pixels.

Terrain (e.g. mountain shadows over fjords and lakes) and building/object shadows can also be difficult to detect automatically. As with cloud shadows spectral tests are generally insufficient and extraneous information from high resolution Digital Terrain Models (DTM), if available, may help in the detection of mountain shadows. Removal of shadows from fixed land-based structures (buildings at the coast, offshore platforms, windmills) and moving objects (ships, even port cranes) is even more problematic and may require algorithms to detect spatial heterogeneity … with the accompanying risk of removing real aquatic processes.

Adjacency effects can contaminate remote sensing data because of violation of the AC assumption that atmosphere and air-water interface reflectance for any target pixel can be calculated using a horizontally uniform water and atmosphere around the target pixel. Adjacency processes include both the “Fresnel land mask” reduction of air-water interface reflectance and the forward scattering of photons from land surfaces into the sensor field of view (Santer and Schmechtig 2000). The latter process gives particularly severe contamination of pixels for near infrared based extrapolative aerosol corrections and for clear water pixels close to vegetated land. Early indications from mass processing of L8 and S2 imagery suggest that adjacency effects are less problematic than was originally expected, possibly because these sensors have SWIR bands that can be used for AC and that are less sensitive to adjacency effects.

The lower **signal:noise ratio** (SNR) of the current generation of high resolution (1-30m) sensors can be critical for water applications. This will be especially problematic for dark waters such as CDOM-rich lakes and open ocean waters, where the noise may be comparable to or greater than the water-leaving radiance itself. The sensor noise will often set a detection limit for parameters such as SPM or CHL concentration. SNR can be improved by spatial binning of data, but obviously at the cost of reducing spatial resolution.

Sensors designed for land applications generally have much **broader and possibly asymmetric spectral bands** than specified for water applications and some spectral variability of water reflectance may be unresolved. A central wavelength approach often adds considerable uncertainty and band-shifting adaptations are therefore required to the standard ocean colour retrieval algorithms (Lee 2009), and for validation purposes.

Panchromatic bands, e.g. available on Landsat-8, provide an extreme case of broad spectral bands. For cases where broadband water reflectance variability is essentially determined by a single parameter, such as particulate backscatter or SPM concentration, it is possible to adopt simple band-sharpening approaches (G. Neukermans, Ruddick, and Greenwood 2012) to effectively exploit the even higher spatial resolution of such bands.

Vicarious calibration and validation are complicated by the reduction in matchups with in situ data arising from the narrow swath and consequent low temporal resolution of data from high spatial resolution sensors. This is particularly critical in the first few years of a mission. The deployment of autonomous instruments on permanent structures is clearly required, e.g. BOUSSOLE (Antoine et al. 2008), MOBY (Clark et al. 2003), AERONET-OC (Zibordi et al. 2009), Smartbuoys (Mills et al. 2003), etc.

5. Conclusions

The public release of free, high resolution (10-30m) data from Landsat-8 and Sentinel-2 opens up the possibility of many new applications in coastal, estuarine and inland waters. Human impacts, for example relating to sediment transport or pollution events, are more visible at such length scales. Some biological processes, such as patchy plankton blooms and floating algae, also become more easily detectable at high resolution. These new data sources also raise new challenges for algorithm developers because of the need to deal with low signal:noise ratio, wide spectral bands, cloud, terrain and object shadows, and spatially resolved (or partially resolved) skyglint and sunglint from surface waves. Traditional ocean colour processing approaches, including strictly pixel-by-pixel atmospheric correction algorithms need to be refined, e.g. including information on a pixel neighbourhood to reduce noise. In fact, while applications and data processing algorithms have been largely driven since the mid-1990s by the medium resolution “ocean colour” sensors, the terminology “ocean colour” no longer covers the majority of aquatic applications of optical remote sensing and it is time to speak more broadly about “water colour”. Finally, the political impact of publicly available high resolution imagery of waters throughout the world may be considerable in regions with environmental problems to hide, e.g. **Figure 6**.

Acknowledgements

This study was funded by the European Community's Seventh Framework Programme (FP7/2007-2013) under grant agreement n° 606797 (HIGHROC project) and by the Belgian Science Policy Office programme under STEREO-III contract SR/00/325 (PONDER project) and FWI contract BL/58/FWI10 (TURBINET project). HIGHROC partners are thanked for useful discussions. USGS and the European Space Agency and European Commission and Airbus DS are acknowledged for the Landsat-8, Sentinel-2 and Pléiades imagery respectively.

References

Antoine, D., P. Guevel, J-F. Desté, G. Bécu, F. Louis, A. J. Scott, and P. Bardey. 2008. "The 'BOUSSOLE' Buoy-a New Transparent-to-Swell Taut Mooring Dedicated to Marine Optics: Design, Tests, and Performance at Sea." *Journal of Atmospheric and Oceanic Technology* 25 (6): 968–989.

Bowman, Malcolm J., and Richard L. Iverson. 1978. "Estuarine and Plume Fronts." In *Oceanic Fronts in Coastal Processes*, edited by Malcolm J. Bowman and Wayne E. Esaias, 87–104. Springer Berlin Heidelberg. doi:10.1007/978-3-642-66987-3_10.

Bresciani, M., D. Stroppiana, D. Odermatt, G. Morabito, and C. Giardino. 2011. "Assessing Remotely Sensed Chlorophyll-a for the Implementation of the Water Framework Directive in European Perialpine Lakes." *Science of The Total Environment* 409 (17): 3083–91.

Chang, C.W, S. V. Salinas, S.C Liew, and Z. P. Lee. 2007. "Atmospheric Correction of IKONOS with Cloud and Shadow Image Features." In , 875–78. IEEE. doi:10.1109/IGARSS.2007.4422936.

Clark, D.K., M.A. Yarbrough, M. Feinholz, S. Flora, W. Broenkow, Y.S. Kim, B. C. Johnson, S.W. Brown, M. Yuen, and J. L. Mueller. 2003. "MOBY, A Radiometric Buoy for Performance Monitoring and Vicarious Calibration of Satellite Ocean Color Sensors: Measurement and Data Analysis Protocols. Chapter 2." http://ntrs.nasa.gov/search.jsp?R=20030063145.

Dekker, A., V. Brando, J. Anstee, S. Fyfe, T. Malthus, and E. Karpouzli. 2006. "Remote Sensing of Seagrass Ecosystems: Use of Spaceborne and Airborne Sensors." In *Seagrasses: Biology, Ecology and Conservation*. Springer.

Dierssen, H. M., A. Chlus, and B. Russell. 2015. "Hyperspectral Discrimination of Floating Mats of Seagrass Wrack and the Macroalgae Sargassum in Coastal Waters of Greater Florida Bay Using Airborne Remote Sensing." *Remote Sensing of Environment* 167: 247–258.

Doron, M., M. Babin, A. Mangin, and O. Hembise. 2007. "Estimation of Light Penetration and Horizontal and Vertical Visibility in Oceanic and Coastal Waters from Surface Reflectance." *Journal of Geophysical Research* 112 (C06003): 1–15.

Franks, P. J. S., and L. J. Walstad. 1997. "Phytoplankton Patches at Fronts: A Model of Formation and Response to Wind Events." *Journal of Marine Research* 55 (1): 1–29. doi:10.1357/0022240973224472.

Gohin, F., B. Saulquin, H. Oger-Jeanneret, L. Lozac'h, L. Lampert, A. Lefebvre, P. Riou, and F. Bruchon. 2008. "Towards a Better Assessment of the Ecological Status of Coastal Waters Using Satellite-Derived Chlorophyll-a Concentrations." *Remote Sensing of the Environment* 112 (8): 3329–40.

Gordon, H.R., and M. Wang. 1994. "Retrieval of Water-Leaving Radiance and Aerosol Optical Thickness over the Oceans with SeaWiFS: A Preliminary Algorithm." *Applied Optics* 33 (3): 443–52.

Hedley, J. D., A. R. Harborne, and P. J. Mumby. 2005. "Technical Note: Simple and Robust Removal of Sun Glint for Mapping Shallow-Water Benthos." *International Journal of Remote Sensing* 26 (10): 2107–2112.

Hochberg, E. J., S. Andrefouet, and M. R. Tyler. 2003. "Sea Surface Correction of High Spatial Resolution Ikonos Images to Improve Bottom Mapping in near-Shore Environments." *IEEE Transactions on Geoscience and Remote Sensing* 41 (7): 1724–1729.

Hu, C. 2009. "A Novel Ocean Color Index to Detect Floating Algae in the Global Oceans." *Remote Sensing of Environment* 113 (10): 2118–2129.

Lacroix, G., K. Ruddick, Y. Park, N. Gypens, and C. Lancelot. 2007. “Validation of the 3D Biogeochemical Model MIRO&CO with Field Nutrient and Phytoplankton Data and MERIS-Derived Surface Chlorophyll a Images.” *JOURNAL OF MARINE SYSTEMS* 64 (1–4): 66–88. doi:10.1016/j.jmarsys.2006.01.010.

Lee, ZP. 2009. “Applying Narrowband Remote-Sensing Reflectance Models to Wideband Data.” *Applied Optics* 48 (17): 3177. doi:10.1364/AO.48.003177.

Matthews, M.W., S. Bernard, and L. Robertson. 2012. “An Algorithm for Detecting Trophic Status (Chlorophyll-A), Cyanobacterial-Dominance, Surface Scums and Floating Vegetation in Inland and Coastal Waters.” *Remote Sensing of Environment* 124: 637–652.

Mills, D.K., R.W.P.M. Laane, J.M. Rees, M.R.V.d. Loeff, J.M. Suylen, D.J. Pearce, D.B. Sivyer, C. Heins, K. Platt, and M. Rawlingson. 2003. “Smartbuoy: A Marine Environmental Monitoring Buoy with a Difference.” In *Building the European Capacity in Operational Oceanography, Proc. Third International Conference on EuroGOOS*, edited by H. Dahlin, N.C. Flemming, K. Nittis, and S.E. Peterson, 311–16. Elsevier Oceanography Series Publication Series 19.

Mumby, P. J., E. P. Green, A. J. Edwards, and C. D. Clark. 1997. “Coral Reef Habitat Mapping: How Much Detail Can Remote Sensing Provide?” *Marine Biology* 130 (2): 193–202.

Neukermans, G., K. G. Ruddick, and N. Greenwood. 2012. “Diurnal Variability of Turbidity and Light Attenuation in the Southern North Sea from the SEVIRI Geostationary Sensor.” *REMOTE SENSING OF ENVIRONMENT* 124 (September): 564–80. doi:10.1016/j.rse.2012.06.003.

Neukermans, Griet, Kevin Ruddick, Emilien Bernard, Didier Ramon, Bouchra Nechad, and Pierre-Yves Deschamps. 2009. “Mapping Total Suspended Matter from Geostationary Satellites: A Feasibility Study with SEVIRI in the Southern North Sea.” *OPTICS EXPRESS* 17 (16): 14029–52. doi:10.1364/OE.17.014029.

Pringle, N., Vanhellemont, Q., and Ruddick, K. 2015. “Cloud and Cloud Shadow Identification for MERIS and Sentinel-3/OLCI.” In . Vol. ESA Special Publication SP-734.

Santer, R., and C. Schmechtig. 2000. “Adjacency Effects on Water Surfaces: Primary Scattering Approximation and Sensitivity Study.” *Applied Optics* 39 (3): 361–75.

Steinmetz, F., P.-Y. Deschamps, and D. Ramon. 2011. “Atmospheric Correction in Presence of Sun Glint: Application to MERIS.” *Optics Express* 19 (10): 9783–9800.

Stumpf, R.P., and J.R. Pennock. 1989. “Calibration of a General Optical Equation for Remote Sensing of Suspended Sediments in a Moderately Turbid Estuary.” *Journal of Geophysical Research* 94 (10): 14363–71.

Toming, K., T. Kutser, A. Laas, M. Sepp, B. Paavel, and T. Nõges. 2016. “First Experiences in Mapping Lake Water Quality Parameters with Sentinel-2 MSI Imagery.” *Remote Sensing* 8 (8): 640. doi:10.3390/rs8080640.

Van Lancker, V., B. Lauwaert, L. De Mol, H. Vandenreyken, A. De Backer, and H. Pirlet. 2013. “Sand and Gravel Extraction.” http://vliz.be/en/imis?module=ref&refid=230574.

Van Mol, B., K. Ruddick, R. Astoreca, Y. Park, and B. Nechad. 2007. “Optical Detection of a Noctiluca Scintillans Bloom.” *EARSeL eProceedings* 6 (2): 130–37.

Vanhellemont, Q., and K. Ruddick. 2014. “Turbid Wakes Associated with Offshore Wind Turbines Observed with Landsat 8.” *REMOTE SENSING OF ENVIRONMENT* 145 (April): 105–15. doi:10.1016/j.rse.2014.01.009.

Vanhellemont, Q., and Ruddick, K. 2016. “ACOLITE For Sentinel-2: Aquatic Applications of MSI Imagery.” In . Vol. SP-740. Prague.

Vanhellemont, Quinten, and Kevin Ruddick. 2015. “Advantages of High Quality SWIR Bands for Ocean Colour Processing: Examples from Landsat-8.” *Remote Sensing of Environment* 161 (May): 89–106. doi:10.1016/j.rse.2015.02.007.

Wang, M., and W. Shi. 2005. “Estimation of Ocean Contribution at the MODIS near-Infrared Wavelengths along the East Coast of the U.S.: Two Case Studies.” *Geophysical Research Letters* 32 (L13606).

Williams, A.E. 2005. “Water Hyacinth-The World’s Most Problematic Weed.” In *Water Encyclopedia*, edited by J.H. Lehr and J. Keeley. Hoboken, NJ, USA: John Wiley & Sons, Inc. http://doi.wiley.com/10.1002/047147844X.sw1116.

Zhu, Z., and C. E. Woodcock. 2012. “Object-Based Cloud and Cloud Shadow Detection in Landsat Imagery.” *Remote Sensing of Environment* 118: 83–94.

Zibordi, G., B. Holben, I. Slutsker, D. Giles, D. D’Alimonte, F. Mélin, J.-F. Berthon, et al. 2009. “AERONET-OC: A Network for the Validation of Ocean Color Primary Product.” *Journal of Atmospheric and Oceanic Technology* 26: 1634–51.

Figures

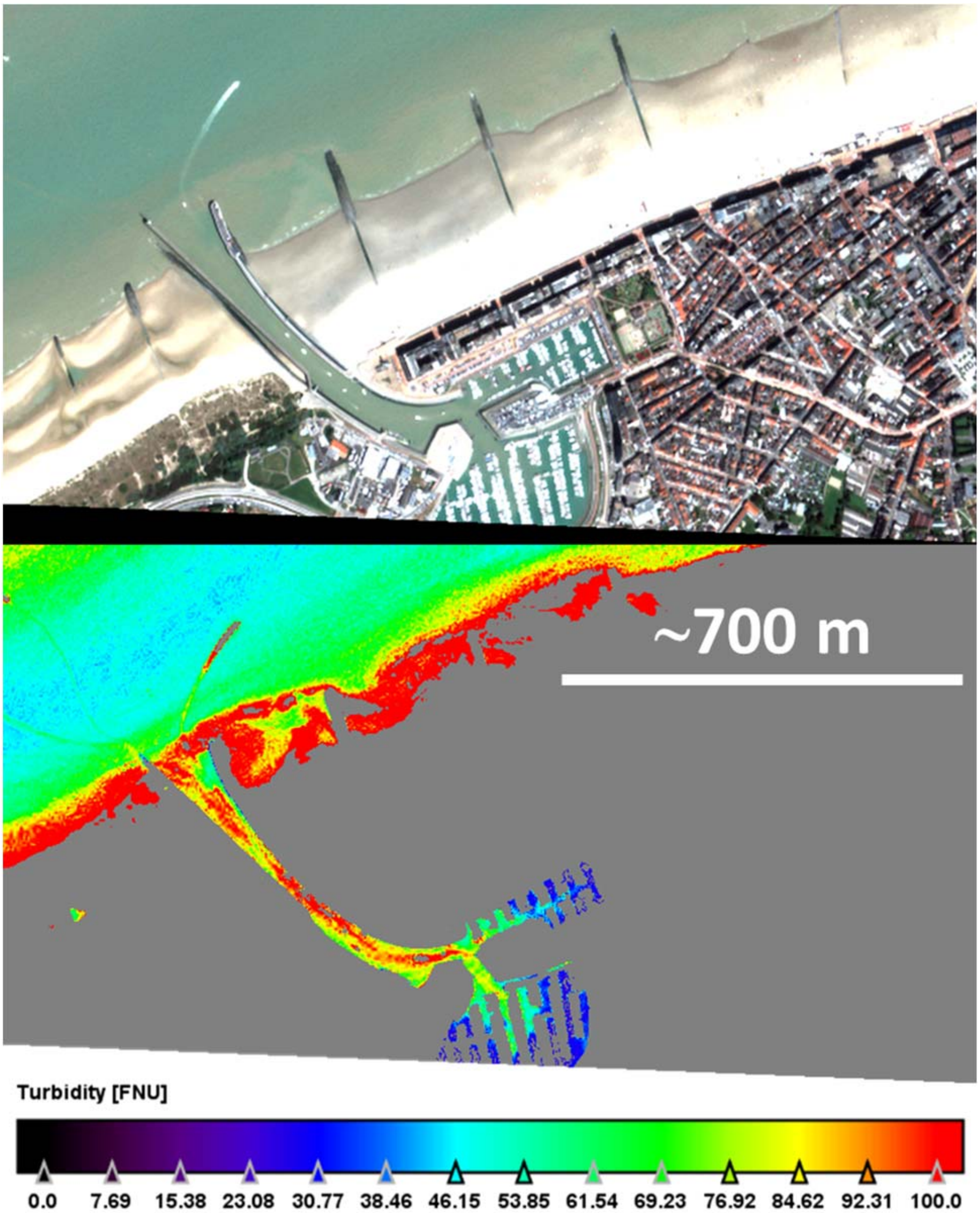

Figure 1. Pléiades imagery on 2014-07-17 of Blankenberge yacht harbour as RGB composite (top) and Turbidity map (bottom), showing suspended sediments entering harbour. Data © CNES (2014), distributed by AIRBUS DS, processed by RBINS using PONDER processor.

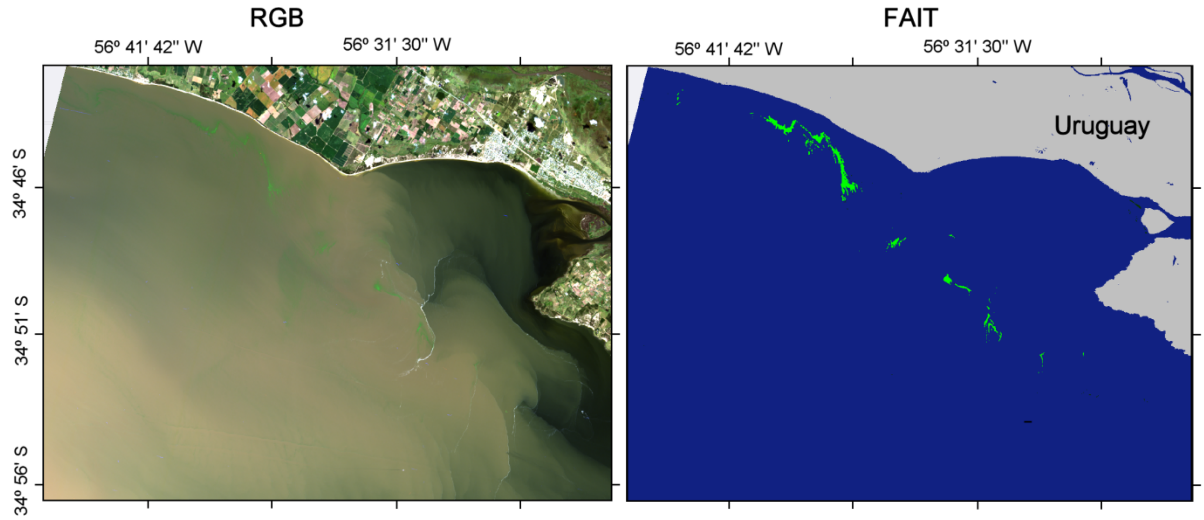

Figure 2. Landsat 8 image of 2015-02-23 West of Montevideo, showing (left) RGB composite of Top of Atmosphere data and (right) pixels in green detected as floating algae or cyanobacteria scum according to the Floating Algae Index modified for Turbid (FAIT) waters – for details of processing see (Dogliotti et al, this volume). Data courtesy of USGS, processed by IAFE using ACOLITE. Many of the patches detected are small (~1 30m pixel wide) and cannot be detected on lower resolution imagery.

Figure 3. Patchy distribution of SPM seen in water near Zeebrugge from (left) Pléiades image of 2014-09-08, data © CNES (2014), distributed by AIRBUS DS, processed by RBINS. and (right) digital camera photo taken from Research Vessel *Belgica* on 2015-04-15. The physical process causing these patches is not well understood.

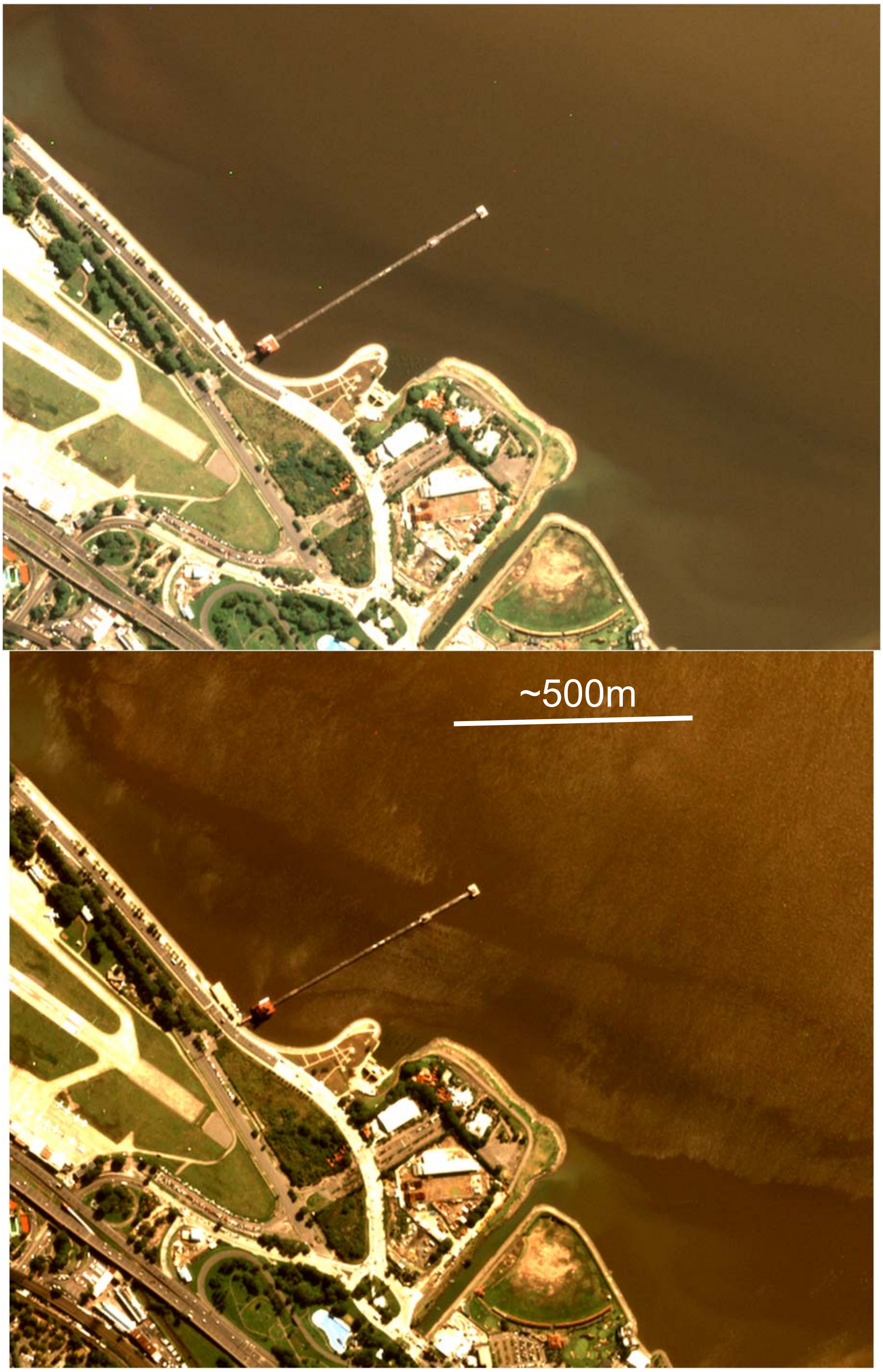

Figure 4. Rayleigh-corrected RGB Pléiades image of the La Plata Estuary and the Fishermans Pier of Buenos Aires on 2016-04-21 taken 62 seconds apart with different viewing zenith angles. The effect of sunglint can be seen clearly in the bottom image and can be precisely calculated. Data © CNES (2016), distributed by AIRBUS DS, processed by RBINS.

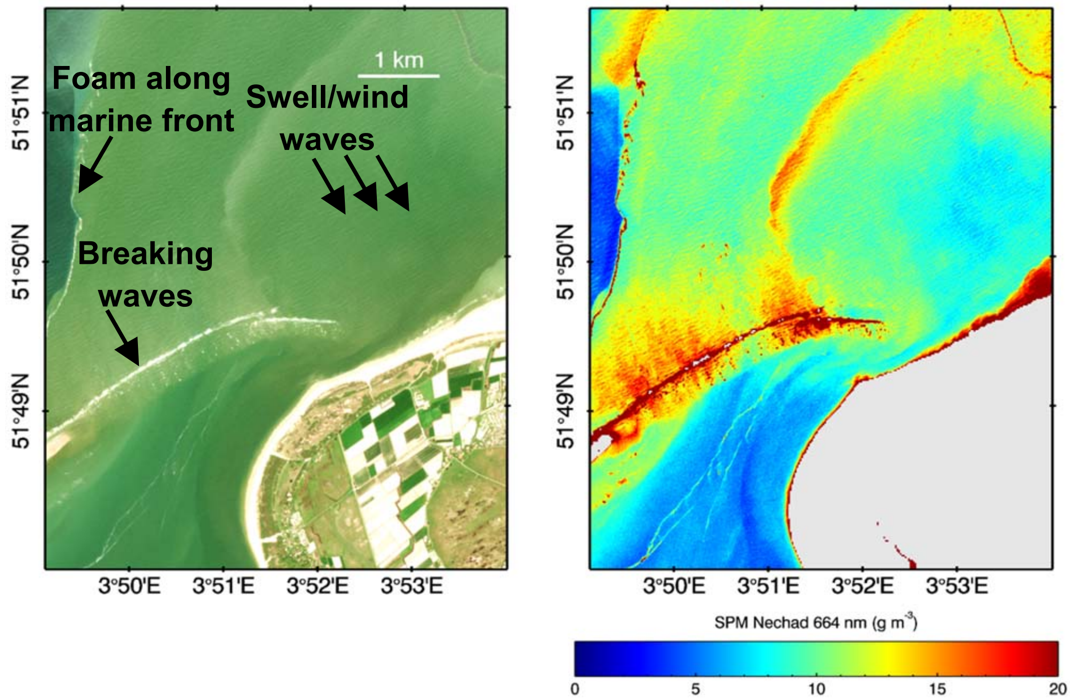

Figure 5. Sentinel 2A image of 2016-05-01 in coastal waters near Goeree showing (left) RGB image with swell waves, breaking wave foam and foam along a front and (right) SPM concentration with corresponding artefacts. Data supplied by ESA, processed by RBINS using ACOLITE.

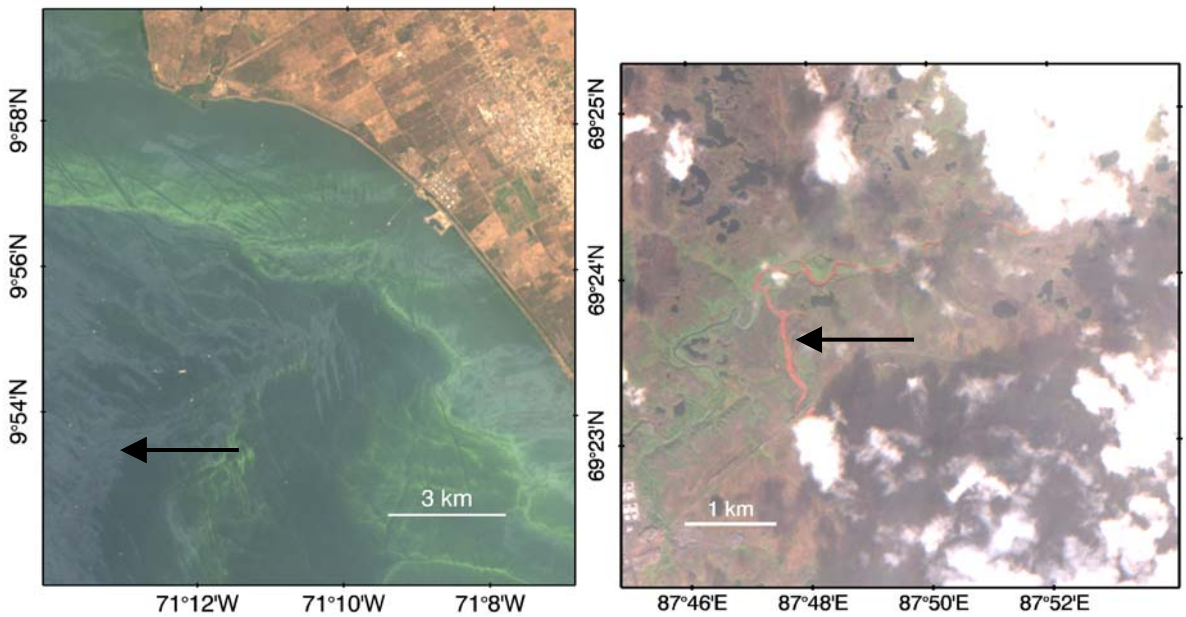

Figure 6. (left) Oil slick from drilling activities (shiny, grey) and Duckweed (bright green) in Lake Maracaibo, Venezuela seen in Landsat-8 image of 27.2.2014; (right) red discolouration of Daldyakan river, Russia seen in Sentinel-2A image of 2016-08-28 – see also “In Siberia, a ‘Blood River’ in a Dead Zone Twice the Size of Rhode Island”, New York Times, 8 Sept 2016. Data supplied by USGS and European Space Agency, processed by RBINS using ACOLITE.